

CHARACTERIZATION OF HIGH ALLOY STEEL PRODUCED VIA ELECTRON BEAM MELTING

Denis Cormier⁺, Ola Harrysson⁺, and Harvey West^{+,++}
⁺Industrial Engineering ⁺⁺Materials Science and Engineering
North Carolina State University
Raleigh, NC 27695-7906

Reviewed, accepted August 19, 2003

Abstract

Electron Beam Melting (EBM) is a direct-to-metal freeform fabrication technique in which a 4 kW electron beam is used to melt metal powder in a layer-wise fashion. As this process is relatively new, there have not yet been any independently published studies of the high alloy steel microstructural properties. This paper describes the EBM process and presents results of microstructural analyses on H13 tool steel processed via EBM.

Introduction

Electron Beam Melting (EBM) is a relatively new direct-metal freeform fabrication process that has been commercialized by Arcam (www.arcam.com). Figure 1 illustrates the basic elements of an Arcam S12 EBM machine. Typically, a 0.1 mm thick layer of metal powder is first spread across the build platform. A 4 kW electron beam gun then preheats the layer using a relatively low beam current and a relatively high scan speed. This preheating step serves two purposes. First, it lightly sinters the metal powder in order to hold it in place during subsequent melting at higher beam powers. Second, it imparts heat to the part that helps reduce the thermal gradient between the melted layer and the rest of the part. By maintaining a more consistent overall part temperature, built-in residual stresses are reduced. Following this preheating step, the layer is melted by increasing the beam power and/or decreasing the scan speed. The build platform is lowered by an amount equal to one layer thickness, a new layer of metal powder is spread, and the process is repeated until the part is complete. Upon completion of the build process, the part is removed from the build chamber. The loose powder supporting the part is removed, and the part is air cooled to room temperature. Bead blasting with silicon carbide, aluminum oxide or other appropriate blast media removes any powder clinging to the part surface. At this point, the as-processed part has a textured surface that resembles a sand casting. If necessary, finish machining of critical part features can be performed.

One advantageous feature of the EBM process is that the loose powder supports all downward-facing surfaces, thus highly complex geometric shapes such as conformal cooling channels are easily built without any need for complex 5-axis programming for collision avoidance. Taminger [1] observed that electron beam melting of metals is very energy efficient and is particularly well suited for processing highly reflective metals such as aluminum that can be difficult to melt with lasers. Lastly, as the entire process takes place in a vacuum, a certain amount of material purification takes place due to the removal of gasses such as those that cause porosity in metal castings.

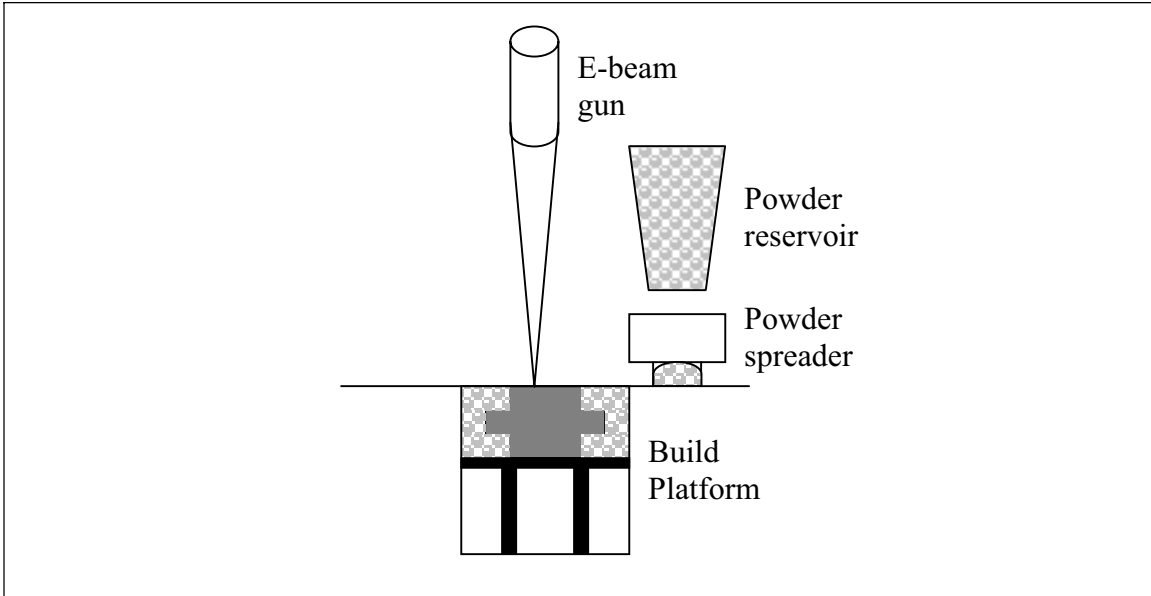


Figure 1 - Layout of Arcam EBM S-12 Machine

During the EBM build process, each slice is divided into two regions – contours and squares. The example in Figure 2 only shows a single contour, however, the user can specify that multiple offset contours be built. The area within a layer that remains after the area of the contours is melted is the bulk area to be melted. Rather than melting all of this area in a left-to-right or spiral scanning pattern, the slicing software subdivides this area into a series of sub-regions called “squares”. In order to evenly distribute heat and to prevent thermal distortions, these squares are melted in a random order that changes from one layer to the next. As is illustrated in Figure 2, squares that are adjacent to a contour are cropped to the shape of the contour. The size of the squares is typically 10 - 15 mm.

At present, there do not appear to have been any independently published studies of the Arcam EBM process. The company states that a wide variety of metal powders can be processed with the process, although Arcam initially chose to concentrate on the use of H13 tool steel alloys for tooling applications. A titanium alloy (Ti6Al4V) has also been developed, and the company is now working on developing parameters for other high-performance alloys. Taminger [1] describes encouraging experiments involving e-beam freeform fabrication of 2219 aluminum alloy in wire form, and Matz [2] also describes unique material properties of a 718 nickel-based superalloy that was fabricated using a similar wire-feed e-beam freeform fabrication process. These studies provide strong evidence that e-beam freeform fabrication is well suited for a wide variety of metal and metal composite materials. The remainder of this paper discusses preliminary results of tests conducted using Arcam’s EBM S12 machine to process H13 tool steel powder.

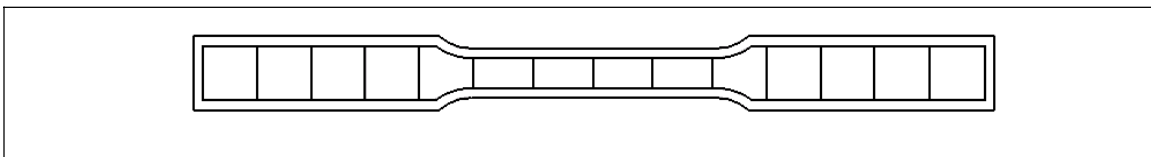


Figure 2 – Illustration of Contours and Squares for a Tensile Test Specimen

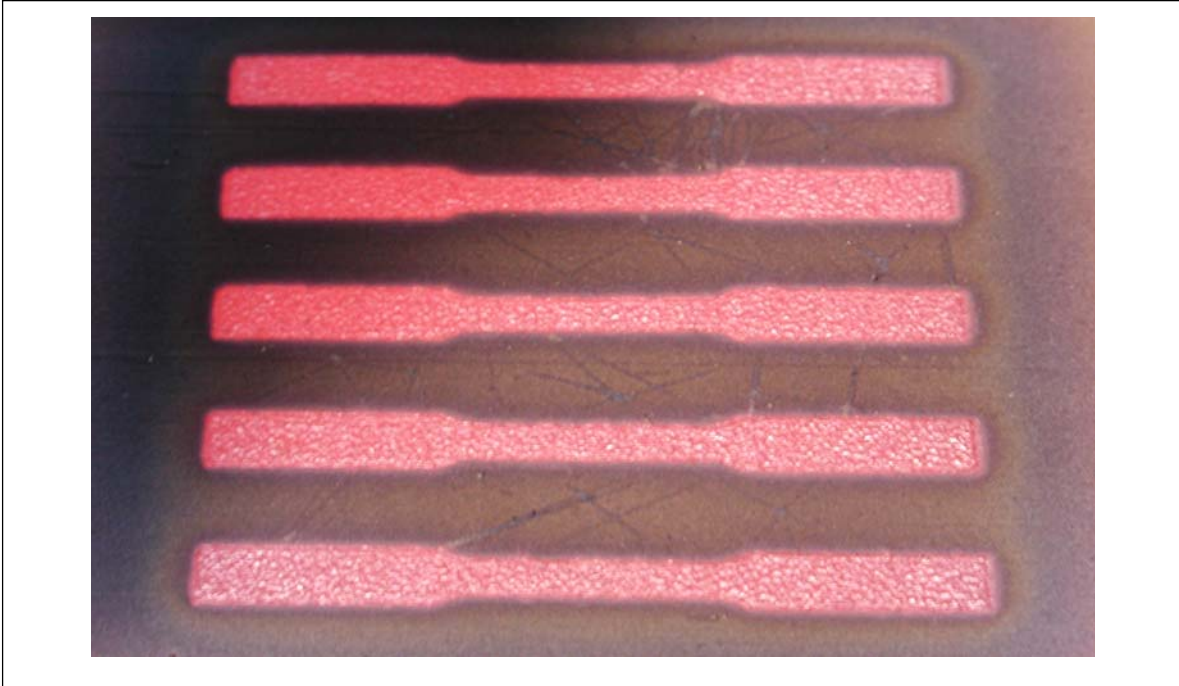


Figure 3 – A Set of Five Subsize Tensile Test Specimens Prior To Powder Removal

Experimental Procedure

In order to begin studying the microstructure and properties of H13 steel produced via EBM, several sets of standard 4-inch sub-size tensile test specimens were fabricated in accordance with ASTM E8 [3] (see Figure 3). Parts were built using the default layer thickness of 0.1 mm. Each layer was preheated 10 times with a scan speed of 10,000 mm/sec and a beam current that was progressively increased from 2 mA on the first scan to 20 mA on the 10th scan. Note that at a scan speed of 10,000 mm/sec, the entire preheating cycle takes a matter of seconds. Following preheating, each layer was melted. A total of two contours were first melted using a beam speed of 100 mm/sec and a beam current up to 20 mA. The squares were then melted at a speed of 500 mm/sec and a beam current up to 20 mA. All processing parameters such as scan speed and beam current can be specified by the user. As is to be expected, the choice of parameter values considerably influences build time and material properties.

In total, three jobs consisting of five specimens each were fabricated using identical build parameters as described above. The first two sets of specimens were removed from the S12 machine immediately upon completion of the job and were rapidly air-cooled. As this is an air-hardening steel, it was hypothesized that rapid air cooling would result in the formation of martensite. The second of these two sets was then annealed in a furnace by heating it to a temperature of 900°C and then allowing it to cool to room temperature at a rate of 22°C/hr. The third set of specimens was allowed to slowly cool to room temperature in the build chamber under vacuum in order to determine whether or not the properties would be affected by the slower cooling rate (without a subsequent anneal).

Prior to preparation of the specimens for microstructural examination, the hardness of the slowly cooled set of specimens was tested. A set of measurements from different samples produced a range of hardness values from 46.0 to 47.3 HRC. This suggested that cooling in the build chamber under vacuum was not slow enough to prevent the formation of martensite. Consequently, samples from this group were not considered for microstructural examination.

One specimen from each remaining group was prepared for microstructural examination. Transverse and longitudinal sections of solid bars were obtained using a water-cooled cutoff wheel and mounted in Bakelite. The surfaces to be viewed were ground on progressively finer grits of silicon carbide paper, rough polished using 6-micron diamond paste, and fine polished with 1 micron and 0.3 micron alumina suspensions. The samples were etched with a 4% solution of nitric acid in methanol. An Olympus inverted stage metallurgical microscope equipped with digital camera was used for optical examination. The microstructure was also viewed using a Hitachi S-3200N Environmental Scanning Electron Microscope (SEM) equipped with an Oxford energy dispersive X-ray spectrometer capable of light element detection.

For the chemical analysis, samples of the H13 powder as well as a section from a fabricated bar were submitted to NSL Analytical Services for chemical analysis. X-ray fluorescence spectroscopy was used to determine the levels of cobalt, chromium, manganese, molybdenum, nickel, silicon, vanadium, and tungsten. The amount of phosphorus present was measured with optical emission spectroscopy, and the amounts of carbon and sulfur were determined via LECO furnace.

Results and Discussion

Chemical Analysis

The results of the chemical composition analysis for the as-processed H13 steel are presented in Table 1. ASTM A681 upper and lower limits [4] for H13 steel are included in the table for reference. Arcam considers its powders to be proprietary at this time, hence composition of the raw powder cannot be included in the table.

Table 1- Chemical Composition of as-processed H13 Steel Versus ASTM A681 Specifications

Element	Minimum Allowable %	Measured %	Maximum Allowable %
Carbon	0.32	0.37	0.45
Manganese	0.20	<0.1	0.60
Phosphorus	0.000	0.011	0.030
Sulfur	0.000	0.005	0.030
Silicon	0.80	1.02	1.25
Chromium	4.75	4.99	5.50
Vanadium	0.80	1.05	1.20
Molybdenum	1.10	1.65	1.75

With the exception of manganese, all alloying elements fall within ASTM limits for H13 steel. One of the interesting challenges with e-beam melting of metal alloys lies in the fact that the process typically takes place in vacuum. Ordinarily, the vaporization of lower melting point alloying elements would be a significant concern. With EBM and similar processes, however, solidification of the melt pool takes place so rapidly that the magnitude of vaporization is quite limited. The degree of vaporization is obviously a function of the processing parameters, and future experiments are planned to help obtain a better understanding of how rapidly the metal solidifies under a given set of conditions.

Hardness

The hardness of both air-cooled and annealed specimens was measured. The air-cooled specimens had hardness values ranging from 48.0 to 50.0 HRC. This provided initial confirmation of the hypothesis that the as-processed material would consist of martensite. As expected, the specimens that were subsequently annealed had HRC values under 20.

Microstructural Analysis

As described previously, samples of both air-hardened and annealed specimens were prepared for inspection via optical microscopy and SEM. Figure 4 shows a micrograph of air-cooled steel produced via the EBM process. For reference, a 500 μm scale is shown. Recall that a layer thickness of 100 μm was used to fabricate this part. As expected, the structure is 100% martensite. It is apparent that the part is virtually 100% dense. Interlayer fusion also appears to be complete.

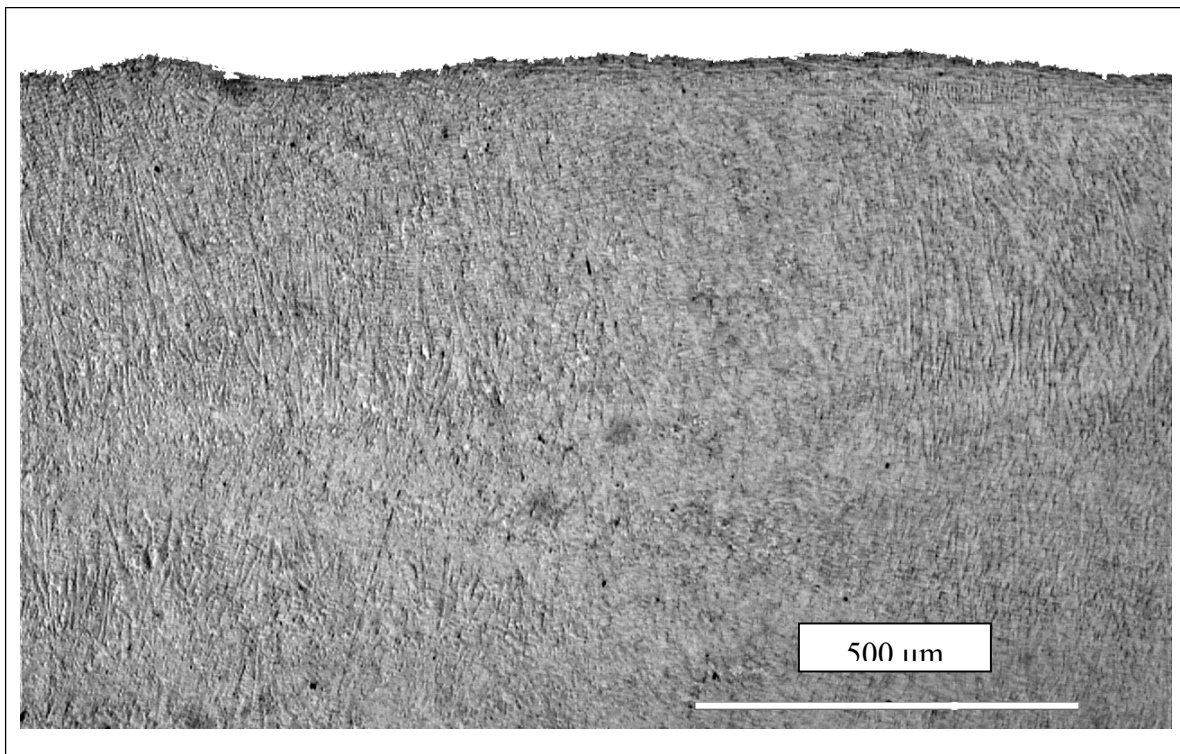


Figure 4 - Microstructure of Air-Cooled H13 Specimen



Figure 5 - Optical Micrograph Showing Local Inhomogeneities

From a metallurgical perspective, a set of interesting localized non-homogeneities were observed at the boundary between the melted contours and interior square regions (see Figure 5). These non-homogenous regions are not visible prior to etching. In an attempt to characterize this non-homogeneity, an X-ray line scan across the region shown in Figure 6 was performed to detect variations in the amounts of C, Si, Mo, V, Cr, and Fe present. As indicated in the spectra to the right of the figure, the chemical composition within the non-homogeneity is essentially identical to what is found in the surrounding matrix. The specimen was immersed in liquid nitrogen to determine if the non-homogeneity might be retained austenite. Unfortunately, this treatment had no effect on the non-homogeneity. Lastly, a Micromet microhardness tester was used to measure hardness within the non-homogeneity. Microhardness testing indicated that the hardness within the non-homogeneity is identical to that of the surrounding martensite. Work is continuing on the characterization of these localized non-homogeneities that are only observed after etching.

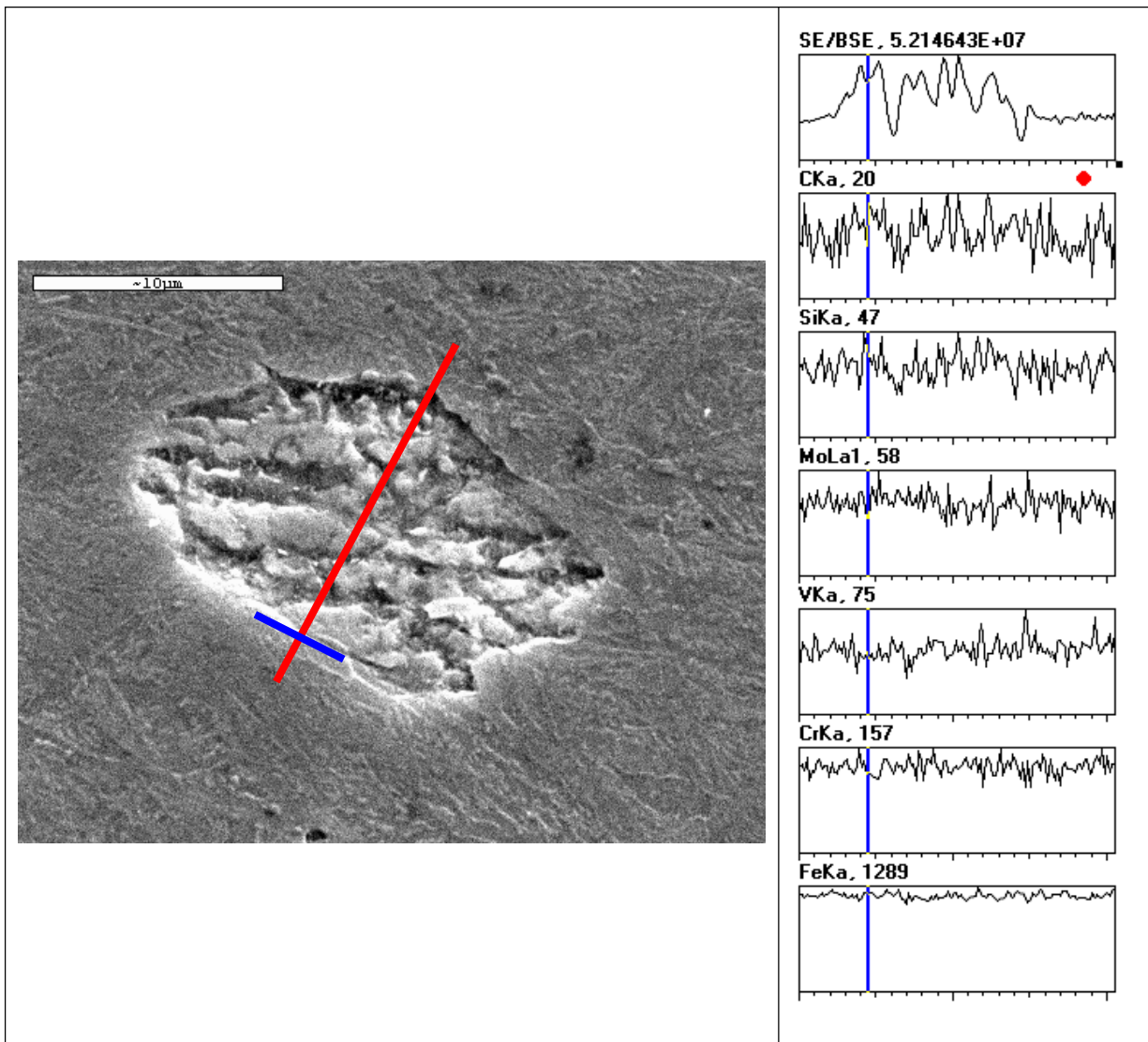


Figure 6 – SEM Photograph Showing Line Scan and Spectra Analysis Across Inhomogeneity

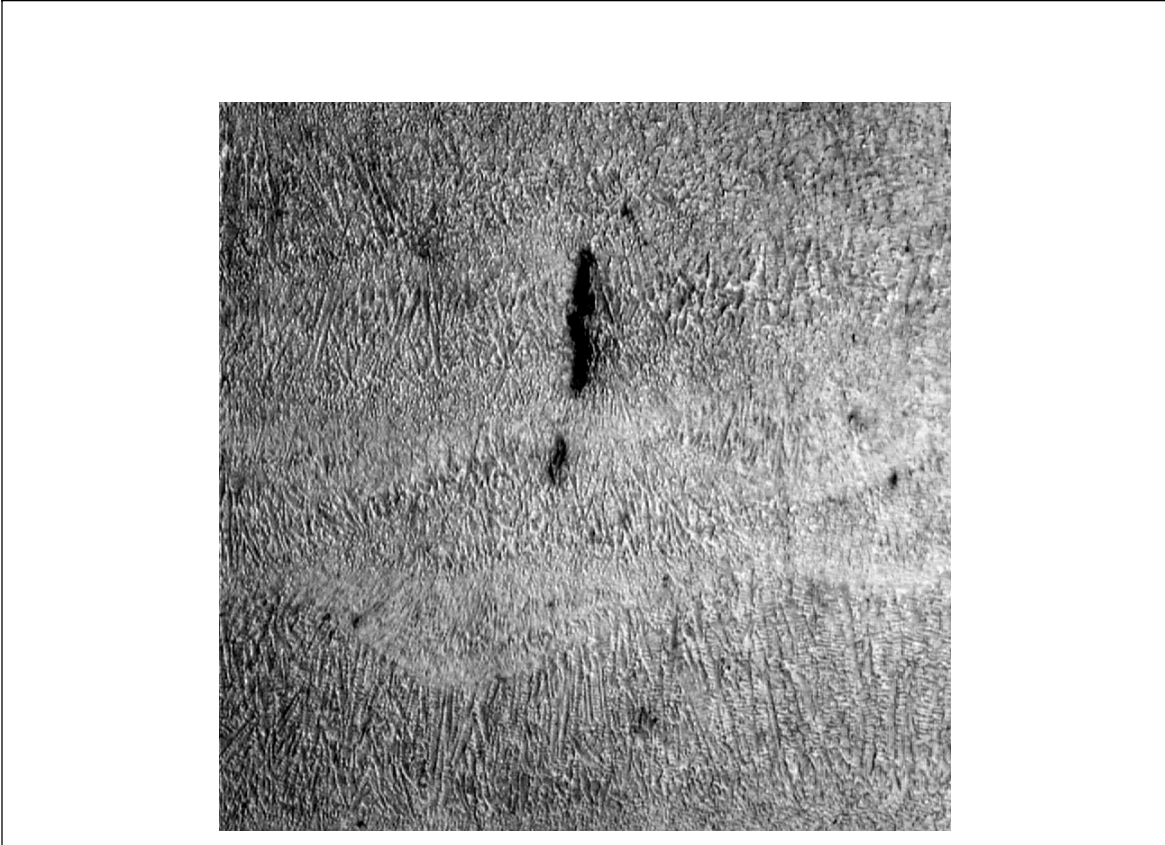


Figure 7 - Optical Micrograph of Intralayer Shrinkage Crack

Although the metallurgical properties were generally quite good under the processing parameters that were used, a small number of isolated shrinkage cracks that were contained within specific layers could be observed. One such crack is shown in Figure 7. As the data presented in this paper is specific to one single set of processing parameters, future experiments will be necessary to determine the effect of processing parameters on microstructure and defects.

Figure 8 shows a micrograph of an annealed specimen taken at 1000X magnification. The microstructure is characteristic of spheroidize-annealed steel. The carbides are distributed both along the grain boundaries and within the grains.

Figure 9 shows an SEM photomicrograph taken at 30,000X magnification that shows the carbide morphology. As shown in Figure 10, an X-ray spot scan of an individual carbide particle (red) was obtained and compared to the X-ray spectrum of the bulk material (black line). Note the increased amounts of C, Mo, Cr, and V and decreased amount of iron present in the red spectrum.

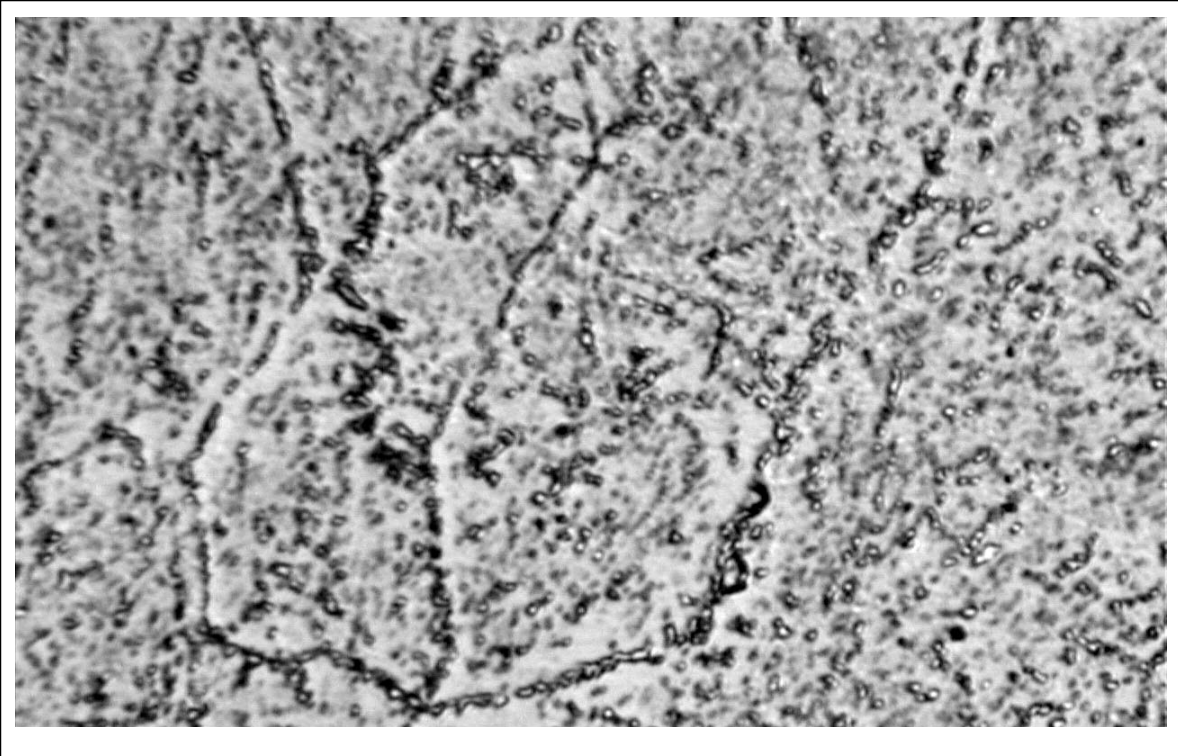


Figure 8 – Optical Micrograph of Spheroidize-Annealed Microstructure (1000X)

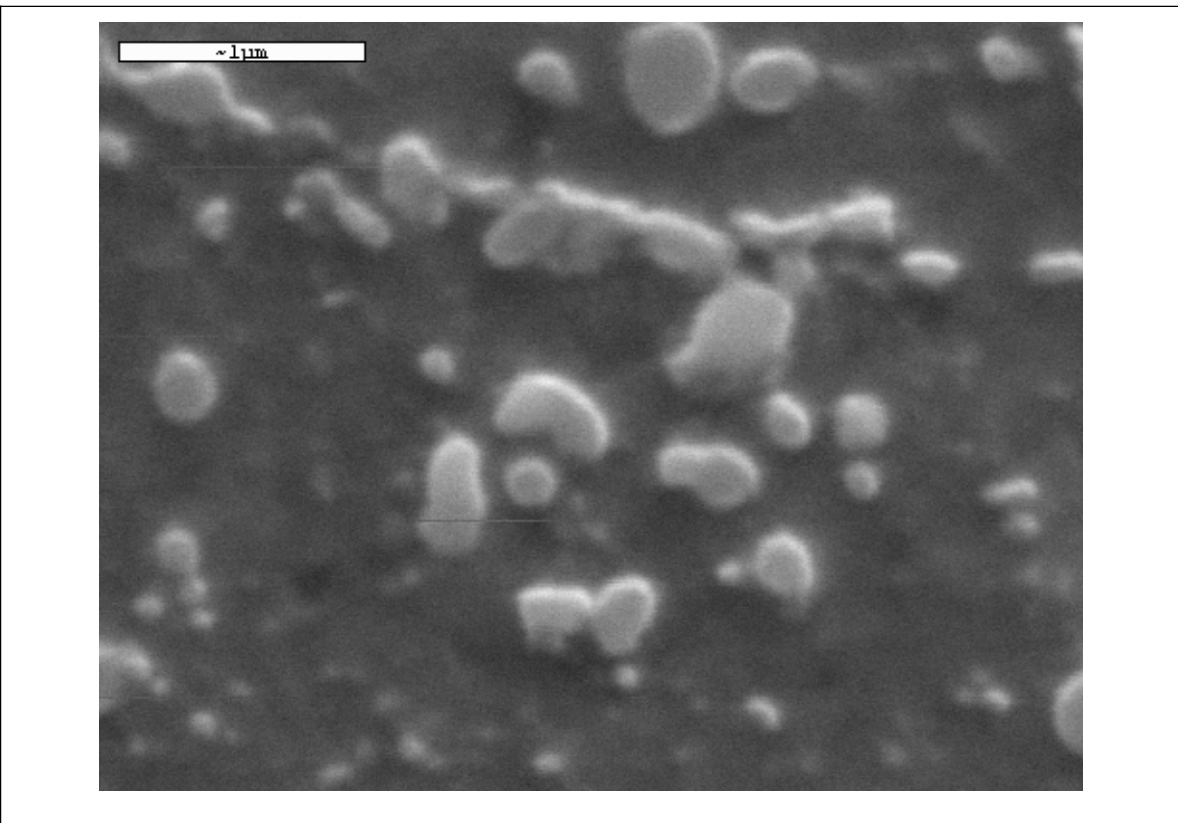


Figure 9 - SEM Photograph of Free Carbides In Annealed Specimen (30,000X)

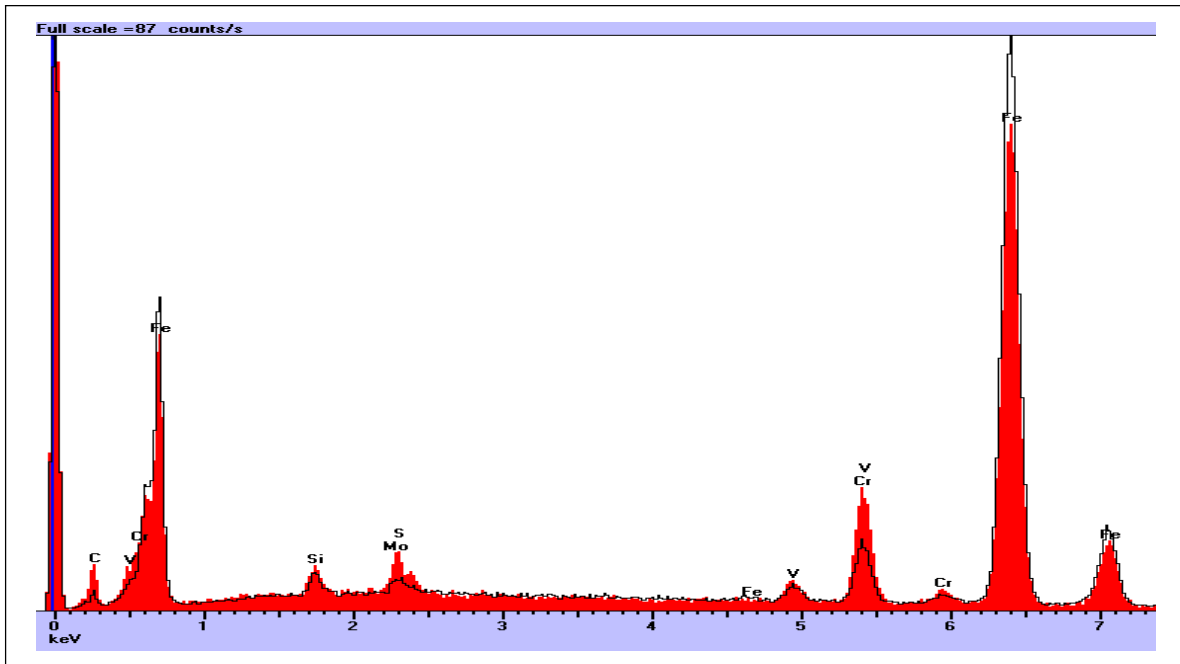


Figure 10 – X-ray Spectra of Bulk Material and Carbide In Annealed Specimen

Conclusions

This paper has presented a microstructural analysis of H13 tool steel produced via the EBM process. As the processing conditions will significantly affect metallurgical properties, the decision was made to conduct this initial study using default processing conditions. Although parameters can be “tuned” for each build according to the part’s geometry, the metallurgical properties obtained using the default parameter values were quite good. The parts exhibited full interlayer bonding with virtually no porosity. The as-processed material was martensite having a hardness of 48-50 HRC. The spheroidize-annealed material also appeared much as expected, with carbides dispersed along the grain boundaries and within the grains themselves.

An interesting observation was the presence of localized non-homogeneities along the boundary between the part’s exterior contours and interior squares. The chemical composition and hardness of these regions is virtually identical to that of the surrounding martensite. Work continues to further characterize these regions.

As one would expect, the selection of processing conditions has a significant influence on build speed as well as mechanical properties. Generally speaking, an increase in build speed is accompanied by a decrease in mechanical properties. The next phase of experimentation (just underway) is to begin studying the relationships between mechanical properties and parameters such as the number of contours, the square sizes, the beam currents (for contours and squares), the beam speed (for contours and squares), the layer thickness, etc. These experiments will help map out the tradeoffs between build speed and metallurgical properties so that the processing parameters can be selected that best meet the needs of the application.

References

- [1] Taminger, K. and Hafley, R. (2002) “Characterization of 2219 Aluminum Produced by Electron Beam Freeform Fabrication” 2002 Solid Freeform Fabrication Symposium Proceedings, pp. 482 - 489

- [2] Matz, J. and Eagar, T. (2002) “Carbide Formation in Alloy 718 during Electron Beam Solid Freeform Fabrication” *Metallurgical and Materials Transactions A*, vol. 33A, pp. 2559 – 2567.

- [3] Standard Test Methods for Tension Testing of Metallic Materials, ASTM E8-01.

- [4] Standard Specification for Tool Steels Alloy, ASTM A681-94.